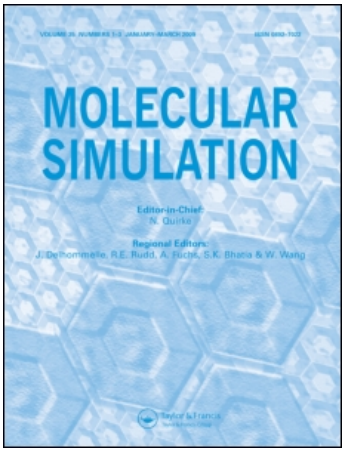

Molecular Simulation
Publication details, including instructions for authors and subscription information:
http://www.informaworld.com/smpp/title~content=t713644482

Molecular Dynamics Simulation of Linear Polymers in a Solvent

W. Smith[a]; D. C. Rapaport[b]
[a] S.E.R.C. Daresbury Laboratory, Theory and Computational Science Division, Cheshire, U.K. [b] Physics Department, Bar-Ilan University, Ramat-Gan, Israel

To cite this Article Smith, W. and Rapaport, D. C.(1992) 'Molecular Dynamics Simulation of Linear Polymers in a Solvent', Molecular Simulation, 9: 1, 25 — 39
To link to this Article: DOI: 10.1080/08927029208048259
URL: http://dx.doi.org/10.1080/08927029208048259

Molecular Simulation, 1992, Vol. 9, pp. 25–39
Reprints available directly from the publisher
Photocopying permitted by license only

MOLECULAR DYNAMICS SIMULATION OF LINEAR POLYMERS IN A SOLVENT

W. SMITH

Theory and Computational Science Division, S.E.R.C. Daresbury Laboratory, Daresbury, Warrington WA4 4AD, Cheshire, U.K.

and

D.C. RAPAPORT

Physics Department, Bar-Ilan University, Ramat-Gan 52900, Israel

(*Received December 1991; accepted January 1992*)

This paper reports a series of simulations of a single linear polymer chain in solution. Both the monomer units and the solvent particles are represented by "beads" which interact via a purely repulsive shifted Lennard–Jones potential; the chains themselves are constructed by linking beads with relatively stiff elastic bonds. The chain lengths range from 8 to 48 beads, and the total system size is between 1000 and 14000 beads. The static and dynamic properties of the polymer chains obtained from long simulations of these systems (over 10^6 timesteps) are discussed, and the size and density dependence of the chain behavior examined.

KEY WORDS: Linear polymers, solvent, chain behaviour

1 INTRODUCTION

A large part of the physics and chemistry of polymers is concerned with the properties of polymer molecules in a solvent. Consequently, the subject has received a great deal of theoretical attention in attempting to explain the behaviour of the solutions in terms of the basic molecular properties of the components. The earliest work was concerned with mathematical treatment of the Rouse–Zimm kind [1, 2], which employed simple models of polymers to derive fundamental relations. However, in more recent years, computer simulation has established itself as an extremely important tool, since it has the advantage of permitting the study of model systems without resort to the severe mathematical approximations essential for more analytical treatments. Most of the early simulations were based on Monte Carlo studies of idealised lattice models, an approach which is computationally efficient, and which continues to yield valuable results in all areas of polymer physics [3, 4]. Off-lattice Monte Carlo simulations are also possible, but are comparatively infrequent because of the computational effort involved.

The main drawback of the stochastic Monte Carlo approach is the absence of time-dependent information; this can only be supplied by a full dynamical treatment. Attempts have been made to exploit lattice models in this area [5], but these have not proved very successful. Hence, despite the added computational cost, there has

been a gradual growth in the use of molecular dynamics (MD) simulation, a trend encouraged by a phenomenal growth in available computing power.

The earliest MD papers to appear exploring the properties of the polymer chain in solution were by Bishop *et al.* [6] and Rapaport [7]. The former used a polymer chain consisting of repulsive spheres, or WCA atoms [8], connected by logarithmic springs, in a solvent also consisting of WCA atoms. The latter constructed chains from hard spheres monomers, with freely-sliding links connecting the monomers, and used hard spheres to represent the solvent. (Henceforth we shall use the term "bead" as a generic term for the monomer units of the chain.) In both cases the system sizes were relatively small: ~ 1000 beads in total being the upper limit in both studies, with only 20 beads in the largest polymer. Both papers examined time-dependent effects, as well as the more usual static properties, thereby setting the agenda for many subsequent studies, but from such short chains it is clearly impossible for the long-chain behavior to be established unambiguously. Perhaps the most interesting result to emerge from these studies was an apparent absence of a solvent effect in the static properties, i.e., the chains possessed essentially the same mean square radius of gyration ($\langle S^2 \rangle$) and end-to-end distance ($\langle R^2 \rangle$), whether isolated or in solution [7]. It is also of interest to recall that Bishop *et al.* observed the same diffusion rate for 5- and 10-bead polymers, and suggested hydrodynamic effects as a possible explanation [6].

Bruns and Bansal [9] used a 9-bead, rigid bonded, Lennard–Jones (LJ) polymer in a solvent of 855 LJ beads under conditions near the LJ triple point. In examining the structural properties of the chain, in particular $\langle R^2 \rangle$, $\langle S^2 \rangle$ and the inertia tensor $T_{\alpha\beta}$ (with α, β denoting x, y, z), and comparing with isolated molecules, they discovered a significant solvent effect. The structure factor $S(q)$ also showed solvent effects at small q. The time-dependent results, when compared with those of Bishop *et al.* [6] gave a much lower diffusion constant, and a negative region in the velocity autocorrelation function (VACF) which was not present in the earlier results. These results served to show that the solvent effects were much more apparent in a liquid-like solvent than in the more rarified solvents of Rapaport and Bishop *et al.*, both for static and dynamic phenomena.

The theme of solvent effects on the static properties of polymers was taken up by Khalatur *et al.* [10] in MD simulations of a 16-bead polymer chain in a solvent of 304 beads and also a multi-chain system of 20 16-bead chains. All potentials used were of modified LJ form, including the chain links. The investigation of dilute polymer solutions with repulsive potentials showed no significant solvent effects on the static structure, but intramolecular (excluded volume) effects increased the molecular size beyond that of the "ideal" (non-interacting, or random walk) chain. In the polymer melt, neighbouring chains screen excluded-volume effects leading to ideal chain behaviour (i.e., the Florey θ point [11]), though this effect was apparently reduced in low density polymers [12]. When attractive forces were introduced the chains contracted. In contrast to Bruns and Bansal's results [9], no convincing evidence of a solvent effect was found, though this may have been a consequence of the different potential function. In the melt the attractive forces were less significant, and the results similar to those for the purely repulsive potential.

Further attention to the question of solvent effects on polymers in solution was given by Smit *et al.* [13]. $\langle S^2 \rangle$ was studied as a function of a parameter λ which scaled the polymer-solvent LJ interaction. A clear dependence of $\langle S^2 \rangle$ on λ was observed, indicating a definite solvent effect. These results led to explicit studies of the "quality" of the solvent [14, 15]. In [14] a study of a 3-arm star polymer constructed out of

19 WCA beads coupled by harmonic springs in a WCA solvent was described. Calculations of $\langle S^2 \rangle$, $\langle R^2 \rangle$ and $T_{\alpha\beta}$ at different densities revealed unambiguous solvent effects. Similar conclusions were drawn for time-dependent phenomena. In [15] a harmonically bonded 8-bead polymer in a 492 bead solvent was studied using a shifted LJ potential for all nonbonded interactions; the interaction between polymer beads and solvent was scaled by the parameter λ. Simulations for different λ values ($0 \leqslant \lambda \leqslant 1.4$) revealed significant solvent effects, both for LJ and WCA potentials, with the former showing a remarkable reduction in $\langle R^2 \rangle$ and $\langle S^2 \rangle$ for small values of λ followed by an increase for larger λ. These were qualitatively accounted for by a "polymer in a sack" model [15].

Luque *et al.* [16] examined several structural and dynamic properties of polymers in solution using conventional LJ potentials between polymer and solvent beads, with different polymer chain lengths and with harmonic and logarithmic springs. Chain lengths ranged from 8 to 20 beads in simulations involving a total of 343 beads. The measured structural properties indicated that the chains were close to the θ point. The time-dependence of $\langle R^2 \rangle$ and $\langle S^2 \rangle$ were also explored, and it was found that the autocorrelation function relaxation times for these quantities generally increased with chain length, and that both a good solvent and a higher density tended to increase the relaxation time. The diffusion constant, D, calculated from the VACF and from the mean-square displacement, was found to be inversely proportional to chain length, in accordance with the free-draining limit applicable in the absence of hydrodynamic interactions.

Though many of these studies looked at dynamic effects, it is true to say that they were exploratory rather than quantitative, and mostly concerned with static properties. This was undoubtedly due to the computational expense, since the long relaxation times of polymer chains and the relatively large systems sizes required to avoid overlap (or even proximity) of a chain and its periodic images imply heavy demands on computing resources. Only recently, with the greater availability of high-performance computing, have the problems been addressed in earnest. In work highly relevant to the study reported here, Dünweg and Kremer [17] have initiated a detailed MD programme of verification of the Zimm model [18] based on studies of chain polymers of 30–60 WCA beads in up to 8000 solvent beads. These computations have established the adequacy of the Kirkwood formula for the short-time diffusion constant and simple dynamical scaling laws, but required the use of Ewald sums [19] to correct the Oseen tensor for long-ranged hydrodynamic effects arising from coupling between the polymer chain and its periodic images. Another recent paper by Pierleoni and Ryckaert [20] reports a study of the relaxation of polymer chains of length 6, 9 and 30 in WCA solvents of 144–690 beads. They have calculated the usual static properties (including $S(q)$) and the associated relaxation times, and verified that the scaling relations are those appropriate for the Zimm model (i.e., including hydrodynamic interactions). This is in contrast to the results of Luque *et al.* [16], who reported Rouse behaviour.

The main conclusions of the work thus far may be summarised as follows. Firstly, the solvent does have a distinct effect on structural properties of polymer chains in solution, and the failure to see this in earlier work was primarily due to low density and/or insufficient sampling. Secondly, the solvent has a strong effect on the dynamic properties, as evidenced by the two studies that have looked for them [17, 20]. But overall, considerably less is known about the dynamics of polymers in solution than the equilibrium structural properties.

In this paper we describe a series of simulations of polymer chains of different lengths (ranging from 8 to 48 beads) in a solvent at two different densities. The total system sizes varied from 1000 to 14000 beads. We have examined the principal conformational properties of the chains, namely end-to-end distance (average and distribution), radius of gyration and persistence length, and dynamical properties such as chain diffusion and the relaxation of the end-to-end distance and radius of gyration.

2 SIMULATION MODEL

The polymer chains are constructed of beads linked by stiff (non-harmonic) springs [21], which restrict the bond length to a relatively narrow range. The solvent fluid consists of beads with the same diameter as those of the chain. The potential functions used are as follows: A repulsive WCA pair potential

$$V_{\mathrm{WCA}}(r) = \begin{cases} 4\varepsilon\left[\left(\frac{\sigma}{r}\right)^{12} - \left(\frac{\sigma}{r}\right)^{6} + \frac{1}{4}\right] & (r \leqslant 2^{1/6}\sigma) \\ 0 & (r > 2^{1/6}\sigma) \end{cases} \tag{1}$$

is used to describe the solvent–solvent, solvent–chain, and the excluded volume part of the chain–chain interactions. The bond interaction is also based on this potential,

$$V_R(r) = V_{\mathrm{WCA}}(d - r) \tag{2}$$

where r is the distance between the bonded beads, and d is a parameter whose value exceeds the maximum permitted bond length and regulates the bond elasticity (the minimum length is set by the WCA potential that maintains excluded volume). The potential V_R is used in this context to produce an effective attraction over a limited range of bead separations; it is nonzero only when $r > d - 2^{1/6}\sigma$. Note that V_R assumes that $r < d$, a condition that the chain finds easy to satisfy.

Standard MD reduced units [24] are used throughout the paper, with the following values: energy ε, length σ, mass m, time $\tau = \sigma(m/\varepsilon)^{1/2}$, temperature ε/k_B, and density σ^{-3}, where k_B is the Boltzmann constant and m the bead mass. Reduced units are indicated by an asterisk. Solvent and chain beads were assigned the same WCA parameters, namely $\varepsilon^* = \sigma^* = m^* = 1$, and all runs were performed at a temperature $T^* \approx 2.0$.

The computations were carried out using an Intel iPSC/860 parallel computer and employed the parallel MD algorithm of Rapaport [22], which is based on the serial "link-cell" algorithm of Hockney and Eastwood [23]. Algorithms of this kind are highly suited to large-scale simulations; as many as 16 nodes were used simultaneously in these calculations, and close to maximal efficiency was achieved (in other words, the computations ran almost 16 times faster than on a single processor). Integration of the equations of motion employed the standard leapfrog algorithm [24]. In each simulation, a chain of the desired length was initially embedded in a simple cubic lattice of WCA beads, which quickly melted as the simulation began. The simulations extended over 1.2×10^6 timesteps, with a timestep value $\Delta t^* = 0.005$. An equilibration period of 2×10^4 timesteps was assumed and the configurational data were subsequently sampled at 100 timestep intervals. Estimates of the error in the calculated structural properties were obtained by the method of Flyvbjerg and Petersen [25].

Table 1 Computed structural parameters for system A ($\rho^* = 0.625$).

Chain length	*System size*	$\langle R^2 \rangle^*$	$\langle S^2 \rangle^*$	*Shape* (A_3)	*Mean bondlength**	*Persistence length**
8	1000	11.9 ± 0.3	2.04 ± 0.03	0.54 ± 0.04	1.0644 ± 0.0001	0.91 ± 0.03
16	1000	29 ± 2	4.8 ± 0.1	0.54 ± 0.08	1.0643 ± 0.0001	0.98 ± 0.05
24	1728	54 ± 4	8.3 ± 0.4	0.5 ± 0.1	1.0644 ± 0.0001	1.16 ± 0.07
32	4096	97 ± 9	14.0 ± 0.9	0.6 ± 0.2	1.0643 ± 0.0001	1.5 ± 0.1
40	8000	127 ± 11	18 ± 1	0.6 ± 0.3	1.0644 ± 0.0001	1.6 ± 0.1
48	13824	110 ± 36	19 ± 2	0.6 ± 0.4	1.0644 ± 0.0001	1.1 ± 0.4
Exponent		1.28 ± 0.11	1.24 ± 0.06			

Two series of simulations were performed: system A with density $\rho^* = 0{\cdot}625$ and system B with $\rho^* = 0.417$. Polymer chains of 8, 16, 24, 32, 40 and 48 beads were studied at each density.

3 RESULTS

3.1 Structural Properties

The computed structural properties for systems A and B appear in Tables 1 and 2.

3.1.1 End-to-end distance

The mean-square end-to-end distance of a polymer chain ($\langle R^2 \rangle$) is defined as the configurational average

$$\langle R^2 \rangle = \langle |\mathbf{R}_{N_b} - \mathbf{R}_1|^2 \rangle \tag{3}$$

where $\mathbf{R}_i$ is the position of the ith bead and N_b is the number of beads in the chain. $\langle R^2 \rangle$ was calculated for all the chains in the A and B systems and was found to increase monotonically with N_b, with the exception of the 48-bead chain of system A, which has a smaller value than the 40-bead chain. This will turn out to be one of several indications of a potential lack of convergence for the longer chains at this relatively high density, and it will be shown later that this can be attributed to the fact that the relaxation times amount to a significant fraction of the total run duration. Theory [1, 2] predicts that $\langle R^2 \rangle$ scales as $(N_b - 1)^{2\nu}$, with $2\nu = 1.18$ for excluded volume chains. By plotting log ($\langle R^2 \rangle$) against log $(N_b - 1)$ we obtain $2\nu = 1.28 \pm 0.11$ for system A and $2\nu = 1.18 \pm 0.03$ for system B. The larger errors for system A reflect the slower convergence of structural properties at the higher density.

Table 2 Computed structural parameters for system B ($\rho^* = 0.417$).

Chain length	*System size*	$\langle R^2 \rangle^*$	$\langle S^2 \rangle^*$	*Shape* (A_3)	*Mean bondlength**	*Persistence length**
8	1000	13.5 ± 0.3	2.19 ± 0.02	0.57 ± 0.03	1.0677 ± 0.0002	1.05 ± 0.02
16	1000	34 ± 1	5.3 ± 0.1	0.56 ± 0.05	1.0684 ± 0.0001	1.12 ± 0.04
24	1728	58 ± 3	9.2 ± 0.3	0.56 ± 0.07	1.0684 ± 0.0001	1.25 ± 0.05
32	4096	79 ± 6	12.5 ± 0.6	0.5 ± 0.1	1.0677 ± 0.0001	1.23 ± 0.09
40	8000	113 ± 9	17.4 ± 0.9	0.6 ± 0.1	1.0677 ± 0.0001	1.4 ± 0.1
48	13824	123 ± 11	20 ± 1	0.5 ± 0.1	1.0675 ± 0.0001	1.3 ± 0.1
Exponent		1.18 ± 0.03	1.18 ± 0.02			

It is of interest to examine the end-to-end distance distribution function $P(R)$, since MD studies of this are relatively uncommon. Our analysis follows that of Bishop and Clarke [26] who used a lattice model. For 3-dimensional random (Gaussian) chains [1, 2]

$$P(R) = 4\pi \left[\frac{3}{2\pi \langle R^2 \rangle} \right]^{3/2} R^2 \exp\left(- \frac{3}{2\langle R^2 \rangle} R^2 \right) \tag{4}$$

For the excluded volume case Mazur [27] proposed the improved functional form

$$P(R) = \left[\frac{\Gamma(5/t)}{\Gamma(3/t)\langle R^2 \rangle} \right]^{3/2} \frac{tR^2}{\Gamma(3/t)} \exp\left(- \left[\frac{\Gamma(5/t)R^2}{\Gamma(3/t)\langle R^2 \rangle} \right]^{t/2} \right) \tag{5}$$

where t is an empirical parameter determined [27] from Monte Carlo simulations to be 2.9. Bishop and Clarke [28] have also shown that this form provides a better fit to the simulation data than the Gaussian form. More recently, however, these authors have shown that the fit at small R is fortuitous, and owes much to the presence of R^2 term that precedes the exponential [26]. The spatial (as opposed to the radial) dependence of the distribution function is given by

$$P(\mathbf{R}) = P(R)/4\pi R^2 \tag{6}$$

which must fall to zero as $R \to 0$ because of excluded volume. This does not occur for either the Mazur or the Gaussian forms. Following the work of des Cloizeaux [29] another form was introduced, namely

$$P(R) = \left[\frac{\Gamma((5 + \theta)/t)}{\Gamma((3 + \theta)/t)\langle R^2 \rangle} \right]^{(3+\theta)/2} \times \frac{tR^{2+\theta}}{\Gamma((3 + \theta)/t)} \exp\left(- \left[\frac{\Gamma((5 + \theta)/t)R^2}{\Gamma((3 + \theta)/t)\langle R^2 \rangle} \right]^{t/2} \right) \tag{7}$$

where the value $\theta = 5/18$ follows from theoretical arguments. This functional form does have the correct limiting $R \to 0$ behaviour. Bishop and Clarke have proposed that $t = 2.5$.

We have examined the validity of these equations for the case of system B. Our results for $P(R)$ are presented in Figure 1(a), where the results for all chain lengths are scaled by the appropriate $\langle R^2 \rangle$. Despite the wide scatter several observations can be made. Firstly, it is already apparent that the Gaussian distribution fails to account for the observed distribution at both extremes. The Mazur and des Cloizeaux distributions are better, though the scatter prevents a judicious choice between the two. Secondly, the failure of all the distribution curves for short chains is strongly evident at small and large R, an expected result since the theory assumes chains with $N_b \to \infty$. The size of the beads in relation to the chain length clearly forces the distribution to zero at some nonzero R, whereas the finite N_b produces similar behaviour at large R. The results for $P(\mathbf{R})$ are shown in Figure 1(b), where, despite the large scatter in the data, it is clear that only the des Cloizeaux function can account for the small-R behaviour (in the limit $N_b \to \infty$). This represents a valuable distinction between the Mazur and des Cloizeaux functions [26].

3.1.2 Radius of gyration

The radius of gyration ($\langle S^2 \rangle$) of a polymer chain (for monomers with unit mass) is

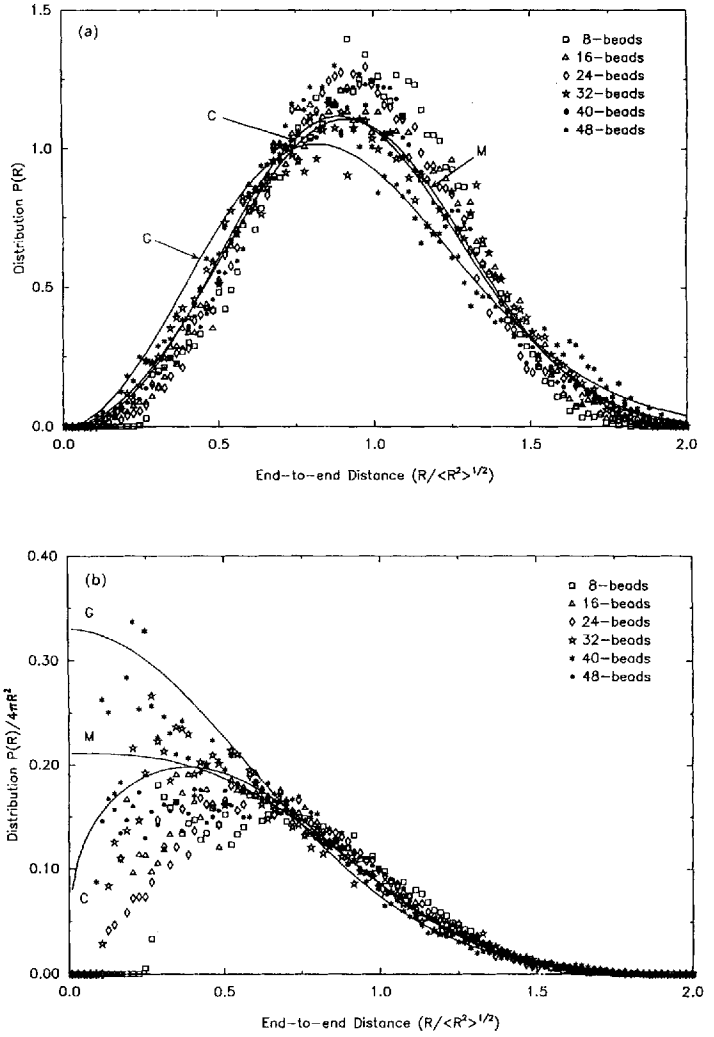

Figure 1 (a) End-to-end distribution function $P(R)$ plotted for all chains in system B ($\rho^* = 0.417$). The continuous lines represent the Gaussian (G), Mazur (M) and des Cloizeaux (C) functions. (b) End-to-end distribution function $P(R)/4\pi R^2$ plotted for all chains in system B. The continous lines are labelled as in (a). Note that the des Cloizeaux curve extrapolates to zero at $R = 0$, as distinct from the Gaussian and Mazur curves. (NB. in both (a) and (b) the plots are scaled so that $\langle R^2 \rangle = 1$).

defined as

$$\langle S^2 \rangle = \left\langle \frac{1}{N_b} \sum_{i=1}^{N_b} |\mathbf{R}_i - \mathbf{R}_c|^2 \right\rangle \tag{8}$$

where R_c denotes the center of mass. The results appear in Tables 1 and 2. The expected behaviour is that $\langle S^2 \rangle$ scales as $(N_b - 1)^{2\nu}$, with ν as before. Plotting

Table 3 Time-dependent properties for System A ($\rho = 0.625$).

Chain length	*Diffusion* $D^* \times 100$	*Relaxation* τ^*_{R2}	*Relaxation* τ^*_R	*Relaxation* τ^*_{S2}
8	1.184 ± 0.006	8.4 ± 0.1	33.88 ± 0.08	6.50 ± 0.03
16	0.432 ± 0.002	25.9 ± 0.3	121.9 ± 0.7	25.6 ± 0.1
24	0.383 ± 0.001	38.3 ± 0.3	222 ± 2	45.9 ± 0.2
32	0.280 ± 0.001	103 ± 2	363.0 ± 0.8	117.6 ± 0.6
40	0.413 ± 0.002	115 ± 1	503 ± 3	142.6 ± 0.4
48	0.392 ± 0.001	178 ± 1	397 ± 1	229.3 ± 0.5
Exponent	0.57 ± 0.20	1.61 ± 0.12	1.41 ± 0.13	1.87 ± 0.09

$\log(\langle S^2 \rangle)$ against $\log(N_b - 1)$ leads to $2\nu = 1.24 \pm 0.06$ for system A and 1.18 ± 0.02 for system B, in reasonable agreement.

The inertia tensor (again, for monomers with unit mass) is

$$T_{\alpha\beta} = \frac{1}{N_b} \sum_{i=1}^{N_b} (\mathbf{R}_i - \mathbf{R}_c)_\alpha (\mathbf{R}_i - \mathbf{R}_c)_\beta \tag{9}$$

Diagonalisation of $T_{\alpha\beta}$ yields the three principal moments of inertia $\{\lambda_i\}$, which can be ordered so that $\lambda_1 \geqslant \lambda_2 \geqslant \lambda_3$. The key feature of the mean 3-dimensional "shape" of the chain is the asphericity A_3 which can be determined from $\{\lambda_i\}$ using the result of Rudnick and Gaspari [30]

$$A_3 = \frac{1}{2} \frac{\langle \Sigma_{i>j} (\lambda_i - \lambda_j)^2 \rangle}{\langle (\Sigma_{i=1}^3 \lambda_i)^2 \rangle} \tag{10}$$

It follows that $A_3 \to 0$ if the chain adopts a spherical conformation and $A_3 \to 1$ if a rod-like conformation is preferred. The calculated values of A_3 are included in Tables 1 and 2. The values are in the range 0.52–0.63 for system A and 0.50–0.60 for system B, indicating ellopsoidal shapes for the chains in solution. The uncertainties prevent deducing any trends in the dependence of A_3 on N_b.

3.1.3 Persistence length

The persistence length P of a polymer chain provides an indication of the degree of "stiffness" of the chain in solution. We have estimated P using the Kratky–Porod model [2], which defines a relationship between $\langle R^2 \rangle$ and the contour length of the chain (L),

$$\langle R^2 \rangle = 2P(L - P[1 - \exp(-L/P)]) \tag{11}$$

where we have assumed that $L = (N_b - 1)\langle r_{\text{bond}} \rangle$ with $\langle r_{\text{bond}} \rangle$ the mean bondlength. P may be obtained by iterative solution of (11). Both P and $\langle r_{\text{bond}} \rangle$ appear in Tables 1 and 2. The persistence length in all cases is of the order of a single bond-length, as expected for freely-jointed flexible chains not subject to any angular constraints. The results appear more consistent for case B, again reflecting the better convergence at lower density.

3.2 Time-dependent Properties

The calculated time-dependent properties are listed in Tables 3 and 4.

3.2.1 Chain diffusion

The diffusion of a single chain in solution is a problem of great current interest. We

Table 4 Time-dependent properties for System B ($\rho = 0.417$).

Chain length	*Diffusion* $D^* \times 100$	*Relaxation* $\tau^*_{R^2}$	*Relaxation* $\tau^*_{\mathbf{R}}$	*Relaxation* $\tau^*_{S^2}$
8	2.618 ± 0.004	2.72 ± 0.03	11.73 ± 0.08	2.42 ± 0.04
16	1.958 ± 0.002	8.18 ± 0.05	29.3 ± 0.2	7.5 ± 0.1
24	1.694 ± 0.006	15.8 ± 0.2	72.8 ± 0.5	14.6 ± 0.1
32	1.073 ± 0.003	31.4 ± 0.4	113.6 ± 0.6	34.9 ± 0.1
40	1.044 ± 0.003	67.7 ± 0.3	150.3 ± 0.5	54.6 ± 0.6
48	0.723 ± 0.002	52.3 ± 0.3	180 ± 1	56.1 ± 0.2
Exponent	0.64 ± 0.10	1.70 ± 0.15	1.50 ± 0.08	1.76 ± 0.12

have calculated the mean-square displacement of the centre of mass for all chains and the results are shown in Figure 2(a) and 2(b). The plots are reasonably linear over the time interval shown. The diffusion constant D was obtained using the Einstein relation

$$\langle |\mathbf{R}(t) - \mathbf{R}(0)|^2 \rangle = 6Dt \tag{12}$$

For system B it is possible to see the expected reduction in diffusion rate with increasing N_b, namely $D_8 > \ldots > D_{48}$. This trend is not apparent for system A, and further confirms earlier observations of poorer convergence at higher density. The diffusion is significantly faster at lower density, as expected. A plot of $\log(D)$ against $\log(N_b - 1)$ provides the exponents 0.57 ± 0.20 (system A) and 0.64 ± 0.10 (system B). From simple scaling and the Stokes law of diffusion it is expected that $D \propto \langle S^2 \rangle^{-1/2}$, so that $D \propto (N_b - 1)^{-\nu}$ with $\nu = 0.59$ (ν being the same exponent as for the configurational exponents); this is what is observed within the (somewhat large) errors calculated here. We note that the longer simulations of Pierleoni and Ryckaert [20] gave an exponent of ~ 0.62.

3.2.2 Configurational relaxation

The time autocorrelation function for R^2 was evaluated using the general formula

$$C_{R^2}(t) = \frac{\langle R^2(t)R^2(0) \rangle - \langle R^2 \rangle^2}{\langle (R^2(0))^2 \rangle - \langle R^2 \rangle^2} \tag{13}$$

The results appear in Figures 3(a) and 3(b). It is apparent that the relaxation is much slower in the higher density system (A). The increase in the relaxation time as N_b increases is also evident in these plots, though for system B we note that the 40-bead chain appears to have a longer relaxation time than the 48-bead chain; in this instance poor convergence is manifest even at the lower density.

In each case we have estimated the relaxation time τ_{R^2}, by fitting the early portion of the correlation function to an exponential form

$$C_{R^2}(t) = \exp(-t/\tau_{R^2}). \tag{14}$$

The relaxation times obtained are shown in Tables 3 and 4. We note the longer relaxation times in case A as compared to B, typically by a factor of ~ 2.5. The length-dependence of the relaxation times has the form $\tau_{R^2} \propto (N_b - 1)^{\alpha}$ and we obtained $\alpha = 1.61 \pm 0.12$ for system A and 1.70 ± 0.15 for system B; scaling requires that $\alpha = 3\nu$. Pierleoni and Rychaert [20] reported a value $\alpha = 1.56$.

The autocorrelation function of the end-to-end distance vector was calculated using

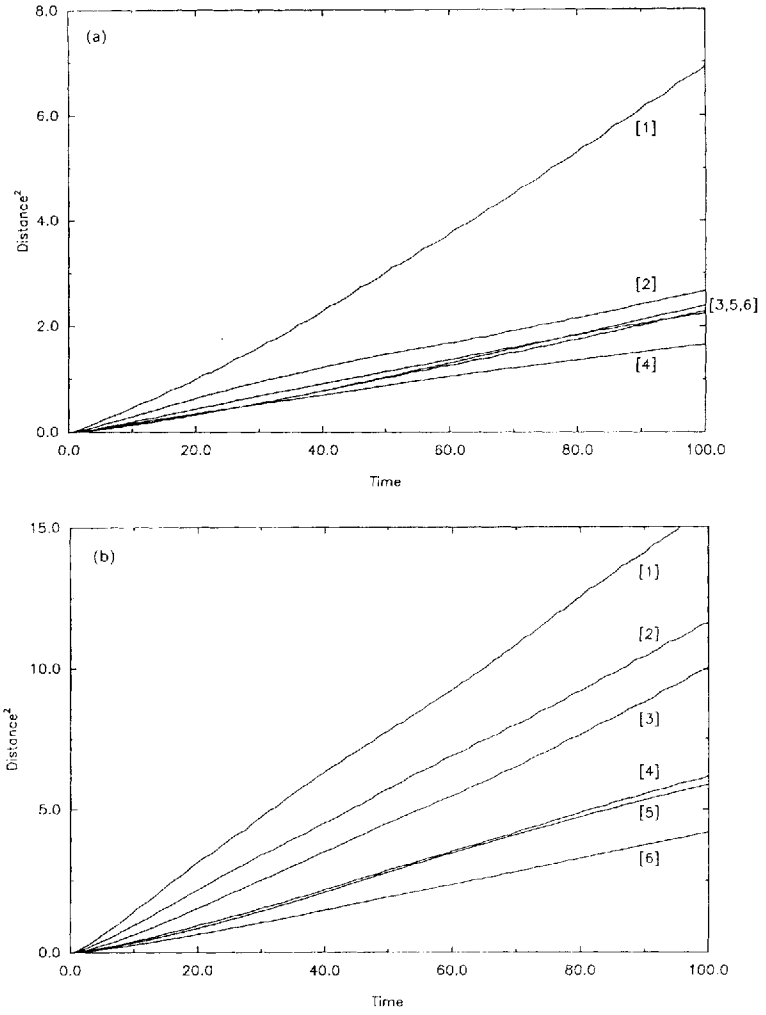

Figure 2 Mean-square displacement *versus* time: (a) for system A ($\rho^* = 0.625$) and (b) system B ($\rho^* = 0{\cdot}417$). [1] ≡ 8 beads, [2] ≡ 16 beads, etc. up to [6] ≡ 48 beads. These and subsequent plots employ reduced units (see Section 2).

the formula

$$C_{\mathbf{R}} = \frac{\langle \mathbf{R}(t) \cdot \mathbf{R}(0) \rangle}{\langle R^2(0) \rangle} \tag{15}$$

The resulting correlation functions are plotted in Figures 4(a) and 4(b). As expected, the rate of relaxation of this vector is much slower than the mean square end-to-end length and slowest of all in the higher density system. The calculated relaxation times $\tau_{\mathbf{R}}$ are listed in Tables 3 and 4. Calculation of the N_b-dependence of this relaxation gives $\alpha = 1.41 \pm 0.14$ and 1.50 ± 0.04 for systems A and B respectively. These exponents are noticeably smaller than those for R^2 and S^2.

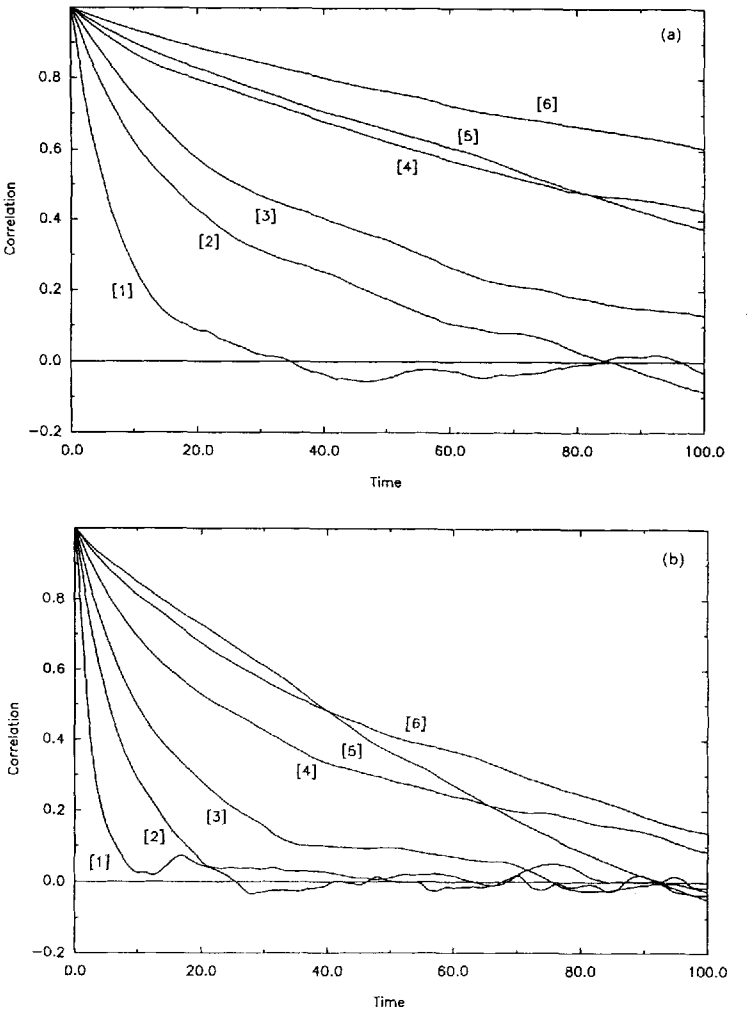

Figure 3 Autocorrelation function ($C_{R^2}(t)$) of the mean-square end-to-end length: (a) for system A and (b) system B. [1] ≡ 8 beads, [2] ≡ 16 beads, etc. up to [6] ≡ 48 beads.

Finally, the time autocorrelation function for S^2 was calculated using a form similar to (13); the results appear in Figures 5(a) and 5(b). Once again the relaxation rate is slower at higher density and tends to drop with increasing chain length, though the longer chains show a departure from the expected ordering in case B. The relaxation times τ_{S^2} appear in Tables 3 and 4; in general they resemble the corresponding values for R^2. The exponents for the N_b-dependence of τ_{S^2} are $\alpha = 1.87 \pm 0.09$ and 1.76 ± 0.12 for systems A and B, again in reasonable agreement with the results for R^2.

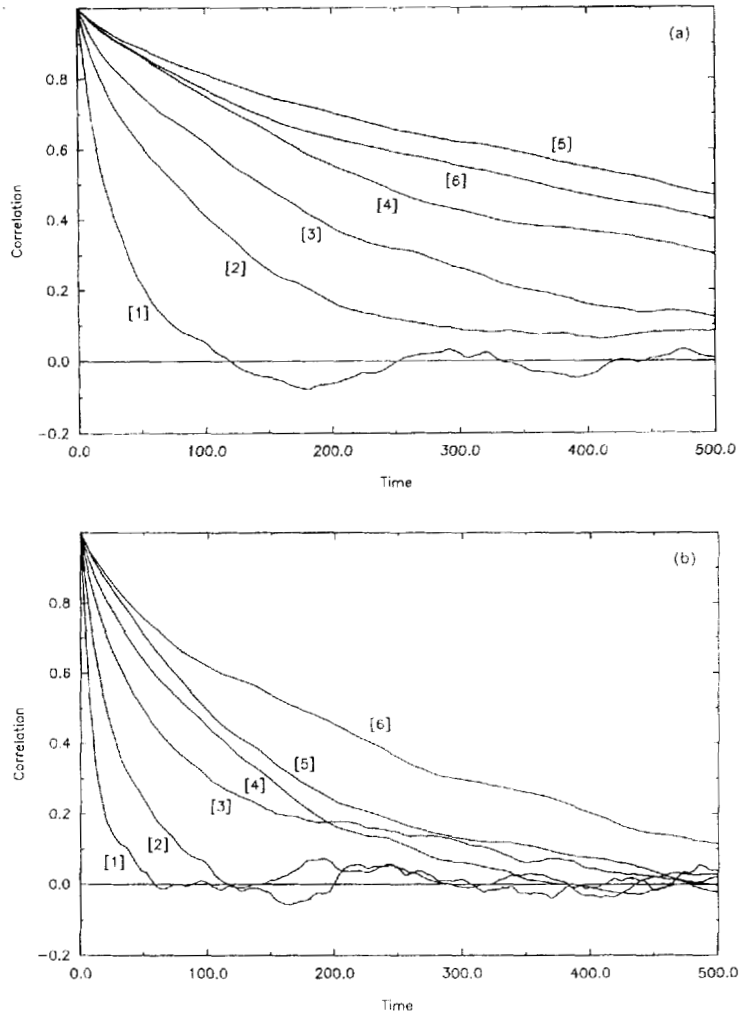

Figure 4 Autocorrelation function ($C_R(t)$) of the end-to-end vector: (a) for system A and (b) system B.

4 DISCUSSION

It is clear from the above results that, despite the length and size of the simulations undertaken, there is still a large measure of uncertainty in some of the calculated properties. The reason for this is easily understood from the temporal length of the simulations in relation to the computed relaxation times. For both R^2 and S^2 the ratio of the simulation time to the relaxation time is of the order 800 (system A) and 2300 (system B) for the shortest 8-bead chain, but these values drop to a mere ~ 30 (A) and ~ 110 (B) for the 48-bead chain. This inevitably implies a severe reduction in the ability to examine adequately the configuration space of the longer chains and, consequently, the degree to which the results can be relied upon (even ostensibly good

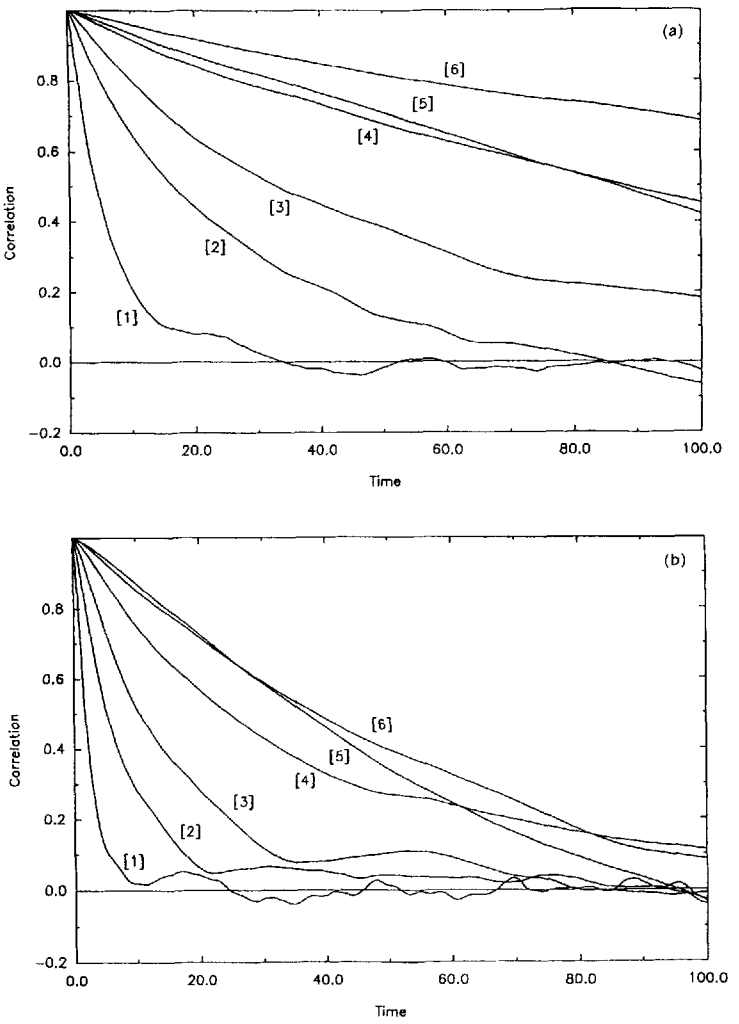

Figure 5 Autocorrelation function ($C_{S2}(t)$) of the mean-square radius of gyration: (a) for system A and (b) system B.

statistics are of little value if the mean value is incorrect). For the longest chains, a simulation of duration sufficient to allow reliable estimation of the dynamical properties (which, at the same time, should also be long enough to provide an adequate sample for estimating the mean configurational properties) would probably have to be an order of magnitude longer, namely 10^7 timesteps. The significance of such uncertainties for the determination of the exponents is also clear. However, on a more optimistic note, the results obtained do represent correct orders of magnitude for these properties, and are useful guides to further simulations.

Subject to the caveats above, we now discuss the calculated physical properties. In general the computed structural properties are reasonable and compare in magnitude

with previous work [6–17, 20]. The N_b-dependence of these properties yields exponents averaging 1.26 in system A and 1.18 in system B. These results are largely what one would expect from previous simulations and available theoretical predictions [1, 2]. The computed relaxation times provide insight into the origin of the likely errors in their computation.

With regard to the time-dependent properties, we note first that the computer diffusion constants are similar to those reported previously. Pierleoni and Ryckaert [20] obtained $10^2 \times D^* = 2.5, 2.0, 0.86$ for chains of length 6, 9 and 30 beads respectively, in simulations at $\rho^* = 0.8$, $T^* = 1.5$. Dünweg and Kremer [17] obtained $10^2 \times D^* = 0.68, 0.55, 0.43$ for chains of 30, 40 and 60 beads and with $\rho^* = 0.864$, $T^* = 1.2$. Our results, which are for systems at lower densities, are more in line with [17] than [20], the latter appearing to be somewhat large. This is possibly because, as in [17], we have simulated systems with a comparatively large number of solvent particles and so the chains are less subject to hydrodynamic coupling between periodic images. This effect has been examined in some detail by Dünweg and Kremer [17], who showed that such effects are clearly important and were able to successfully correct for them in the analysis. The larger uncertainties in our results unfortunately prevent us drawing any quantitative conclusions about this effect here.

The relaxation times τ_{R^2}, $\tau_{\mathbf{R}}$ and τ_{S^2} computed from our simulations provide exponents comparable with [20], where the exponent of $\alpha = 1.55$ was proposed to account for the N_b-dependence. Our exponents for τ_{R^2} are higher than this (1.61 and 1.70), but agree within the calculated margin of error. The $\tau_{\mathbf{R}}$ exponents (1.41 and 1.50) are lower, but reasonably close. It would seem therefore that our results support a Zimm model for time-dependent processes, in agreement with [17, 20] and in contrast to [16].

Comparing the results for the two densities studied here, it appears that the relaxation times are 2 to 3 times longer in the higher density system. At the even higher density studied in [20] (i.e., $\rho^* = 0.805$) the times are an order of magnitude longer than those obtained here. The relaxation times associated with chain conformation are clearly extremely sensitive to changes in solvent density.

5 CONCLUSIONS

In this paper we have attempted to examine the number dependencies of structural and time-dependent properties of a chain polymer in solution. The results are in agreement with other published results, but because of extremely large relaxation times for the longer chains, precise numbers have not been obtained in all cases. We have also shown that the time-dependent properties are in line with the Zimm model and that the timescales of all measured properties increase with density.

An important aspect of this work has been the application of parallel processing to the study of polymers. This has permitted comparatively large simulations to be undertaken cost effectively. Such methods will become essential given the emerging awareness of the magnitude of the task confronting the simulator of polymer systems.

Acknowledgments

The Daresbury Advanced Research Computing Group is thanked for sponsoring DCR on a visit to Daresbury Laboratory, where this work was undertaken, and for time on the Intel iPSC/860 parallel computer. M. Bishop is thanked for instructive comments on section 3.1.1.

References

[1] R.B. Bird, C.F. Curtiss, R.C. Armstrong and O. Hassager, *Dynamics of Polymeric Liquids*, Wiley, New York (1987) Vol. 2, Ch. 15.

[2] M. Doi and S.F. Edwards, *The Theory of Polymer Dynamics*, Clarendon Press, Oxford (1986).

[3] K. Kremer and K. Binder, "Monte Carlo simulations of lattice models for macromolecules", *Comput. Phys. Reports*, **7**, 259 (1988).

[4] K. Binder, "Computer simulation of macromolecular materials", *Colloid and Polymer Sci*, **266**, 871 (1988).

[5] P.H. Verdier and W.H. Stockmayer, "Monte Carlo calculations of the dynamics of polymers in dilute solution", *J. Chem. Phys.*, **36**, 227 (1962).

[6] M. Bishop, M.H. Kalos and H.L. Frisch, "Molecular dynamics of polymeric systems", *J. Chem. Phys.*, **70**, 1299 (1979).

[7] D.C. Rapaport, "Molecular dynamics study of a polymer chain in solution", *J. Chem. Phys.*, **71**, 3299 (1979).

[8] J.D. Weeks, D. Chandler and H.C. Andersen, "Role of repulsive forces in determining the equilibrium structure of simple liquids", *J. Chem. Phys.*, **54**, 5237 (1971).

[9] W. Bruns and R. Bansal, "Molecular dynamics study of a single polymer chain in solution", *J. Chem. Phys.*, **74**, 2064 (1981).

[10] P.G. Khalatur, Yu. G. Papulov asnd A.S. Pavlov, "The influence of solvent on the static properties of polymer chains in solution", *Molecular Physics*, **58**, 887 (1986).

[11] P.J. Florey, *Statistical Mechanics of Chain Molecules*, Interscience (1969).

[12] M. Bishop, M.H. Kalos and H.L. Frisch, "The influence of attractions on the static and dynamic properties of simulated single and multichain systems", *J. Chem. Phys.*, **79**, 3500 (1983).

[13] B. Smit, A. van der Put, C.J. Peters, J. de Swaan Arons, and J.P.J. Michels, "The influence of solvent quality on the static properties of a linear polymer: A molecular dynamics study", *Chem. Phys. Lett.*, **144**, 555 (1988).

[14] B. Smit, A. van der Put, C.J. Peters, J. de Swaan Arons and J.P.J. Michels, "The influence of the density of the solvent on the static and dynamic properties of star polymers", *J. Chem. Phys.*, **88**, 3372 (1988).

[15] B. Smit, K.R. Cox and J.P.J. Michels, "The influence of the quality of the solvent on the properties of a polymer. A thermodynamic model and molecular dynamics simulation", *Molec Phys.*, **66**, 97 (1989).

[16] J. Luque, J. Santamaria and J.J. Freire, "Molecular dynamics of chain molecules in solution. Static and dynamic properties", *J. Chem. Phys.*, **91**, 584 (1989).

[17] B. Dünweg and K. Kremer, "Microscopic verification of the Zimm model by molecular dynamics simulation", *Phys Rev. Lett.*, **66**, 2996 (1991).

[18] B.H. Zimm., "Dynamics of polymer molecules in dilute solution: viscoelasticity, flow birefringence and dielectric loss", *J. Chem. Phys.*, **24**, 269 (1956).

[19] C.W.J. Beenakker, "Ewald sum of the Rotne–Prager tensor", *J. Chem. Phys.*, **85**, 1581 (1986).

[20] C. Pierleoni and J-P. Ryckaert, "Relaxation of a single chain molecule in good solvent conditions by molecular dynamics simulation", *Phys. Rev. Lett.*, **66**, 2992 (1991).

[21] D.C. Rapaport, "Large scale molecular dynamics simulation using vector and parallel computers", *Comput. Phys. Reports*, **9**, 1 (1988).

[22] D.C. Rapaport, "Multi-million particle molecular dynamics II. Design considerations for distributed processing", *Comput. Phys. Comm.*, **62**, 217 (1991).

[23] R.W. Hockney and J.W. Eastwood, *Computer Simulation Using Particles*, McGraw-Hill, New York (1981).

[24] M.P. Allen and D.J. Tildesley, *Computer Simulation of Liquids*, Clarendon Press, Oxford (1987).

[25] H. Flyvbjerg and H.G. Petersen, "Error estimates on averages of correlated data", *J. Chem. Phys.*, **91**, 461 (1989).

[26] M. Bishop and J.H.R. Clarke, "Investigation of the end-to-end distance distribution function for random and self-avoiding walks in two and three dimensions", *J. Chem. Phys.*, **94**, 3936 (1991).

[27] Mazur, J., "On the limiting shape of the distribution function of lengths of a single polymer molecule with excluded volume effects", *J. Chem. Phys.*, **43**, 4354 (1965).

[28] M. Bishop and J.H.R. Clarke, "Brownian dynamics study of the end-to-end distribution function of star and linear polymers in different regimes", *J. Chem. Phys.*, **91**, 3721 (1989). Also "Brownian dynamics study of the end-to-end distribution function of two dimensional linear chains in different regimes", *J. Chem. Phys.*, **91**, 6345 (1989).

[29] J. des Cloizeaux, "Lagrangian theory for a self avoiding random chain", *Phys. Rev.*, **A10**, 1665 (1974).

[30] J. Rudnick and G. Gaspari, "The shapes of random walks", *Science*, **237**, 384 (1987).